Electrical characteristics and influence of the air-gap size in a trielectrode plasma curtain at atmospheric pressure

2009 J. Phys. D: Appl. Phys. 42 045205

(http://iopscience.iop.org/0022-3727/42/4/045205)

IOP PUBLISHING JOURNAL OF PHYSICS D: APPLIED PHYSICS

J. Phys. D: Appl. Phys. **42** (2009) 045205 (7pp) doi:10.1088/0022-3727/42/4/045205

Electrical characteristics and influence of the air-gap size in a trielectrode plasma curtain at atmospheric pressure

R Sosa[1,3], D Grondona[2,3], A Márquez[2,3], G Artana[1,3] and H Kelly[2,3]

[1] Laboratorio de Fluidodinámica, Universidad de Buenos Aires, Av. Paseo Colón 850, 1063, Buenos Aires, Argentina

[2] Instituto de Física del Plasma, CONICET—Dto de Física, FCEN, Universidad de Buenos Aires, Ciudad Universitaria, Pab. I, 1428, Buenos Aires, Argentina

Received 22 October 2008, in final form 11 December 2008
Published 15 January 2009
Online at stacks.iop.org/JPhysD/42/045205

Abstract

A study of the electrical characteristics of the trielectrode plasma curtain (TPC) discharge is presented. The influence of the air-gap size (for a fixed value of the inter-electrode distance) on the discharge behaviour has been exhaustively studied. The TPC discharge is based on the combination of a dielectric barrier discharge (DBD) with a corona discharge (CD) in a three electrode system, and basically it consists of the 'stretching' of a pure DBD by the action of a negative CD generated between the active electrode of the dielectric barrier and a remote third electrode. It was found that the general trend of the electrical characteristic curves (the average discharge current and the streamer frequency as functions of the AC and DC biasing voltages) was very similar for all the air-gap values considered. Our results indicate that the development of the TPC discharge requires two conditions: (a) the presence of a positive cycle of a well-developed DBD together with a CD where the remote electrode acts as the cathode and (b) a voltage drop between the DBD electrode and the remote electrode high enough to obtain an average electric field in the gap that must exceed a minimum average electric field value in the streamer channel necessary for its propagation across the gap ($\approx$6.3 kV cm^{-1} in our experimental conditions).

(Some figures in this article are in colour only in the electronic version)

1. Introduction

The development of non-thermal plasma sources at a high pressure (typically, atmospheric pressure) for plasma processing presents considerable practical interest, because it avoids expensive vacuum systems and batch processing of work-pieces. These plasmas mostly include corona discharges (CDs) [1], dielectric barrier discharges (DBDs) [2] and atmospheric pressure glow discharge (OAUGDP^{TM} [3]). In practice, these sources have been employed in microelectronics [4], surface modifications [5], light sources [6], surface sterilization [7], gas decontamination [8] and flow control [9].

Devices based on DC CDs with two active electrodes allow establishing ionized regions with considerable air gaps but they present some drawbacks, such as problems related to ignition, spark transition and non-uniform distribution of the discharge along the electrodes side length. The AC DBD devices [2] can overcome some of the quoted CD difficulties, but the ionization in these kinds of devices has been in general restricted to the vicinity of the electrodes resulting in ionized air gaps of a few millimetres length.

In a previous work [10], the development of a trielectrode plasma curtain (TPC) discharge that can be sustained over a long time, over inter-electrode air gaps up to 20 mm and with electrodes length of $\sim$15 cm in the transversal direction was presented. The discharge was based on the combination of a DBD with a CD in a three electrode system, and basically it resulted from the 'stretching' of a pure DBD discharge by the action of a CD discharge generated between the active electrode of the DBD and a remote third electrode. The TPC is an extension of a sliding discharge [11–13], in which a considerable part of the dielectric surface is replaced by an air

[3] Member of CONICET.

gap. The electrodes geometry and the discharge characteristics of the TPC make it appropriate for several applications in which a gas flow through the discharge is required. In both cases (sliding or TPC) it was found that a long discharge was generated during the positive cycle of the DBD discharge, and besides it had a pulsed nature, being composed of repetitive streamers that were uniformly distributed along the whole electrode length, and propagated along the inter-electrode gap with an average velocity of $\sim 2 \times 10^7\,\mathrm{cm\,s^{-1}}$, with a mean electric field at the streamer head of $\sim 120\,\mathrm{kV\,cm^{-1}}$ and a total particle number of $\sim 5 \times 10^8$ at the streamer head.

In this work, we present a study of the electrical characteristics of the TPC discharge analysing the influence of the air-gap size (for a fixed value of the inter-electrode distance) on the discharge behaviour.

2. Experimental arrangement

The schematic of the electrode layout is shown in figure 1. The electrode arrangement consisted of two flat aluminium foils (electrodes 1 and 3) of 50 μm thickness, 25 mm width and 150 mm length in the z direction (see figure 1), air-exposed and flush mounted on two poly-methyl methacrylate dielectric surfaces with 4 mm width. There is a third electrode (electrode 2) that was completely covered with an epoxy resin (not air-exposed) with 50 μm thickness, 5 mm width and 150 mm side length in the z direction, located on the opposite side of the dielectric surface holding electrode 1. The specific positions of the electrodes relative to the dielectric plates are indicated in figure 1. D indicates the distance between the electrodes 1 and 3 edges, while d indicates the air-gap size (hence $l = D - d$ is the extension of the dielectric surface from electrode 1 edge). The length d was variable in the experiment but the D value was kept constant at 30 mm. In this way, it was possible to evaluate the role of the relative dielectric and air-gap lengths in the discharge.

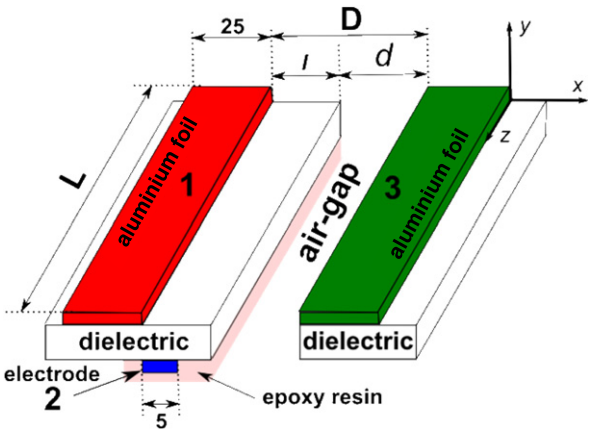

Figure 1. Schematic of the electrode layout (distances are indicated in mm).

In figure 2 the electrical block diagram of the experimental set-up is presented. The electric circuit consisted of a positive variable DC and an AC power supply (continuous voltage V_{DC} in the range 0–20 kV and an alternating peak-to-peak voltage V_{AC} in the range 0–23 kV) connected in series to electrode 1. This biasing scheme allowed measuring the DBD current (I_{DBD}) and the TPC current (I_{TPC}) in each branch of the circuit. These current measurements were performed by connecting electrodes 2 and 3 through 50 Ω resistances to the ground and registering the voltage drop on these resistances. The AC power supply consisted of a function generator coupled to an audio-amplifier (of 700 W) that fed a high voltage transformer coil [14]. In practice, there was an optimal matching frequency, established by the resonance between the transformer inductance and the stray capacity of the electrode arrangement, including the wire connections. For our circuit geometry, the optimum excitation AC frequency was $f_{ac} = 5.6$ kHz. The instantaneous voltage applied to electrode 1, $V(t)$, was measured with a HV probe (1000 × /3.0 pF/100 MΩ). These electrical signals were registered by using a four-channel digitizing oscilloscope with an analog bandwidth of 60 MHz and 1 Gs s^{-1} sampling rate.

It is worth mentioning that the positive DC source could be replaced by a negative variable DC source connected to

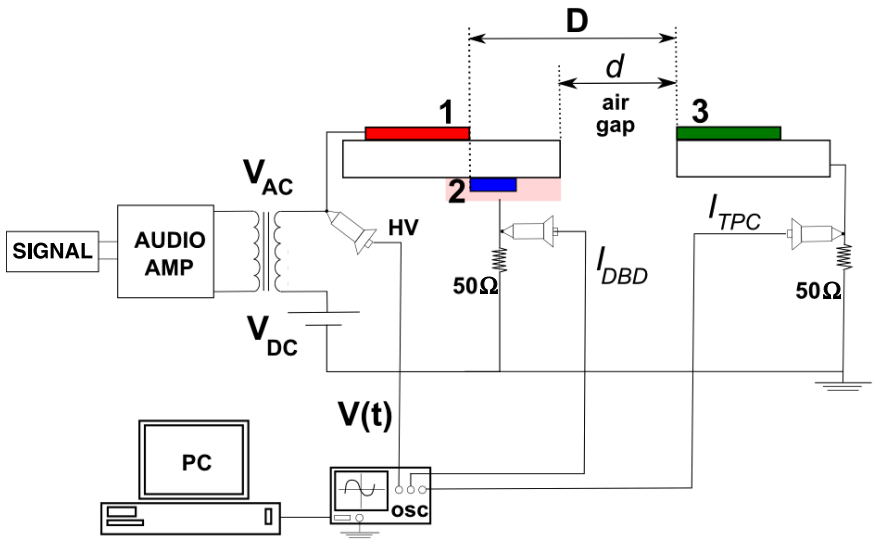

Figure 2. Electrical block diagram of the experimental set-up.

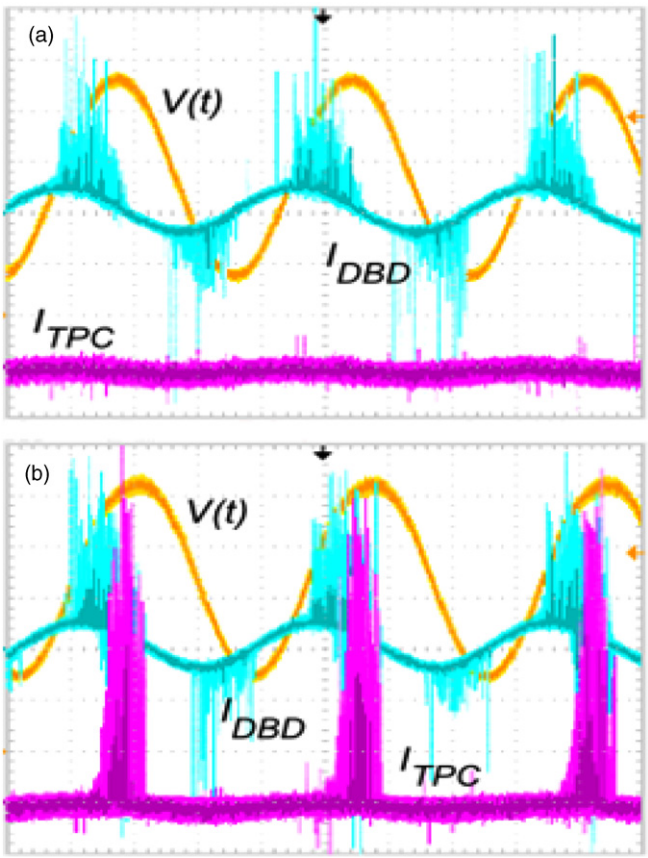

Figure 3. Typical waveforms of $V(t)$, I_{TPC} and I_{DBD} for $d = 15$ mm, $V_{\mathrm{AC}} = 20$ kV and $V_{\mathrm{DC}} = 12$ kV (a) and $V_{\mathrm{DC}} = 16$ kV (b). Current scale 10 mA div^{-1}, voltage scale 5 kV div^{-1}, time scale 50 μs div^{-1}.

electrode 3 without altering the discharge behaviour. However, this biasing mode did not allow in our case the registering of I_{TPC}, because the DC power sources had their own ground connection.

3. Experimental results

In figure 3 typical waveforms of $V(t)$, I_{TPC} and I_{DBD} are presented for $d = 20$ mm, $V_{\mathrm{AC}} = 20$ kV and $V_{\mathrm{DC}} = 12$ kV (a) and $V_{\mathrm{DC}} = 16$ kV (b). Figure 3(a) corresponds to a well-developed DBD discharge between electrodes 1 and 2 (the onset of the DBD discharge appears for $V_{\mathrm{AC}} = 10$ kV for our electrode geometry), showing its characteristic peaks during both AC voltage cycles. However, the absence of peaks in the I_{TPC} waveform indicates that no TPC discharge was established in this case. Figure 3(b) corresponds to a higher value of V_{DC}, allowing the 'turning on' of the TPC discharge. In this situation a train of current pulses can be seen in the waveform of I_{TPC}. Note that the I_{TPC} pulses appear only during the positive cycle of the DBD discharge. The waveforms of figure 3 were acquired with a persistence of 1 s in the oscilloscope display; hence, the number of current peaks displayed in each waveform corresponds to about 5×10^3 cycles of the AC voltage.

As was mentioned in the previous section, the TPC discharge was similarly developed when the positive DC source connected to electrode 1 (see figure 2) was replaced by a negative DC source of the same value connected to electrode 3. However, no TPC discharge could be produced by connecting a positive DC source to electrode 3. It was also found that the presence of electrode 2 (which allows establishing the DBD between electrodes 1 and 2) is essential for the existence of the TPC discharge, because it cannot be developed only by applying a voltage drop between electrodes 1 and 3 (in this case, an unstable and non-uniform plasma sheet was produced).

Figures 4(a) and (b) show photographs of the discharge. The images correspond to an exposure time of 2 s, for $V_{\mathrm{DC}} = 17$ kV and $d = 20$ mm, for two different values of V_{AC}. Figure 4(a) was obtained for $V_{\mathrm{AC}} = 11$ kV (a value slightly above the DBD threshold), and it can be seen that the discharge presents a non-uniform structure that is concentrated in a small number of tufts oddly distributed along electrode 1. Also there is some evidence of a bead-like structure along electrode 3, which was reported in the past by Peek [15] as negative corona instability. Figure 4(b) was obtained for $V_{\mathrm{AC}} = 17$ kV, and in this condition the number of tufts was considerably increased covering practically the whole side length of electrode 1, resulting in an almost uniform plasma structure that filled the inter-electrode gap with a bluish light. The discharge 'slides' along the dielectric surfaces, 'bridging' the air gap between them. We defined this last case as a well-developed TPC. A similar discharge structure was also observed in a two-electrode parallel plate and coplanar configuration of the OAUGDP$^{\mathrm{TM}}$ [3, 16].

To derive some meaningful information on the discharge characteristics in terms of the V_{DC} and V_{AC} values, the following procedure was adopted. By setting the oscilloscope in the average acquisition mode, an average waveform of the current signals (I_{TPC} and I_{DBD}) over 128 samples was acquired. Then, to ignore the reactive component of the current (present even without the discharge), these statistically averaged signals were time averaged over one period of the AC voltage to finally obtain the average current values of I^m_{TPC} and I^m_{DBD}. The uncertainty in the average current values was estimated to be $\pm 50\,\mu$A, mainly due to statistical fluctuations.

In figures 5(a) and (b) we present I^m_{TPC} as a function of V_{DC} with V_{AC} as a parameter and for $d = 10$ mm and 20 mm, respectively. The cases $V_{\mathrm{AC}} = 9$ and 11 kV correspond to a non-well-developed discharge, as shown in figure 3(a). For $V_{\mathrm{AC}} \geqslant 13$ kV (the TPC regime) the discharge current in both cases increases with V_{AC} up to a value for which sparking is produced. This behaviour was found for all the range of d values investigated.

To illustrate the influence of d on the discharge behaviour, in figure 6 I^m_{TPC} as a function of V_{DC} with d as a parameter and for $V_{\mathrm{AC}} = 13$ kV and $V_{\mathrm{AC}} = 19$ kV is presented. It can be seen that within the experimental uncertainties the curves are quite similar, and the only influence of d that can be observed is a slight increase in the current for the largest V_{DC} values. Within the whole range of investigated parameter values (V_{DC}, V_{AC} and d) I^m_{DBD} remained almost constant, with a small value of $I^m_{\mathrm{DBD}} \sim 100\,\mu$A. Since the plasma curtain takes place only during the positive cycle of the DBD discharge, the average positive DBD (I^+_{DBD}) current has been evaluated as a function

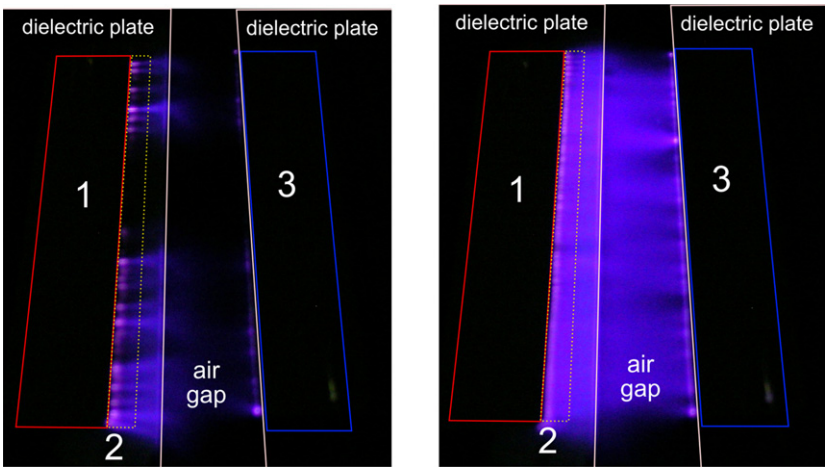

Figure 4. Photographs of the discharge for $d = 20$ mm, $V_{DC} = 17$ kV and $V_{AC} = 11$ kV (a) and $V_{AC} = 17$ kV (b).

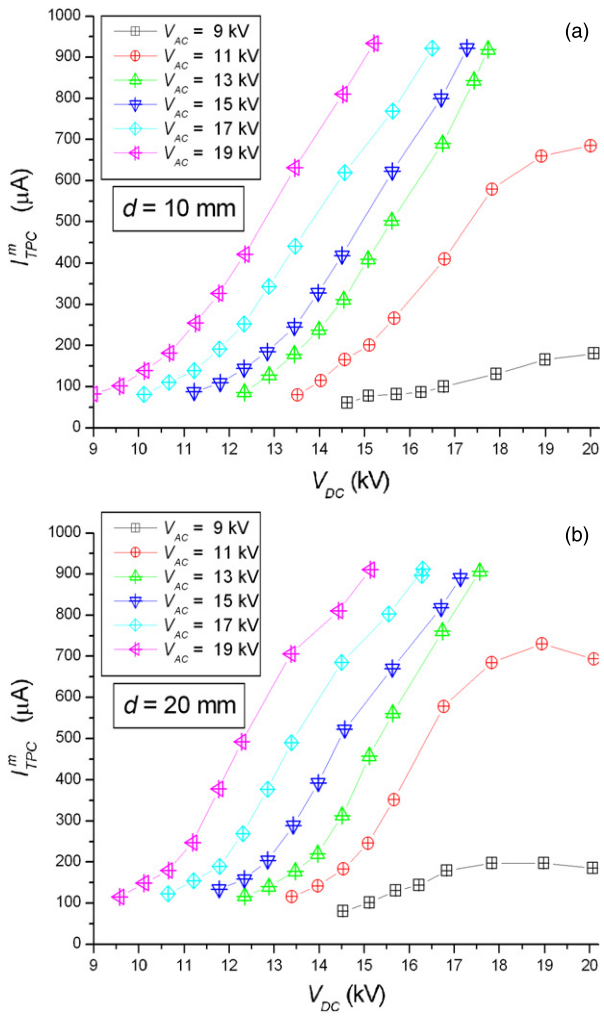

Figure 5. I^m_{TPC} as a function of V_{DC} with V_{AC} as a parameter for $d = 10$ mm (a) and $d = 20$ mm (b).

of d, V_{DC} and V_{AC} within the whole range of the investigated values. It was found that I^+_{DBD} resulted almost independent of d and V_{DC}, but depending on the V_{AC} value. This means that the increase in the I^m_{TPC} value as a function of V_{DC} (for the given values of d and V_{AC}) shown in figure 5 is not related to an increase in I^+_{DBD}. On the other hand, for fixed values of d and V_{DC} the increase in I^m_{TPC} with V_{AC} could be associated with an increase in the I^+_{DBD}. In the cases shown in figure 6, I^+_{DBD} reached a value of 100 μA for $V_{AC} = 13$ kV and 250 μA for $V_{AC} = 19$ kV.

Another important feature of the discharge behaviour is the number of current pulses generated during the discharge. This number was represented by an averaged frequency that was obtained directly from the trigger frequency of the oscilloscope. For practical reasons, the I_{TPC} waveform was selected to obtain the frequency, because in this current signal the alternating reactive current component is relatively small, resulting in a well-defined frequency value. Since this frequency fluctuated somewhat in time (the pulses were not purely periodic), we registered several frequency values of the oscilloscope (around 20 values) during a large time interval (~100 s) and finally calculated the statistical average value (f_s). The associated statistical uncertainties in f_s were not larger than 20%. It is important to mention that the f_s value depended on the selected amplitude of the pulses, which in turn were controlled by the trigger level of the oscilloscope. We thus decided to select a medium-amplitude trigger level, so as to register most of the pulses produced, but rejecting low-amplitude pulses that could be confused with the electrical noise of the discharge. In figures 7(a) and (b) f_s is shown as a function of V_{DC} with V_{AC} as a parameter and for $d = 10$ mm and 20 mm, respectively. It can be seen that f_s increases with V_{DC}, up to a value of $f_s \sim 200$ kHz where sparking is produced. The behaviour of f_s with the discharge parameters is quite similar to that found with I^m_{TPC} (compare figures 5 and 7), and it was found for all the range of d values investigated. The f_s upper value was also found to be dependent on the electrode side length: additional experiments performed with different electrode side lengths showed that f_s scaled almost linearly with that length (L).

In figure 8 f_s as a function of V_{DC} with d as a parameter and for $V_{AC} = 13$ kV and $V_{AC} = 19$ kV is presented. Although the general behaviour of f_s with V_{DC} is similar to that found with

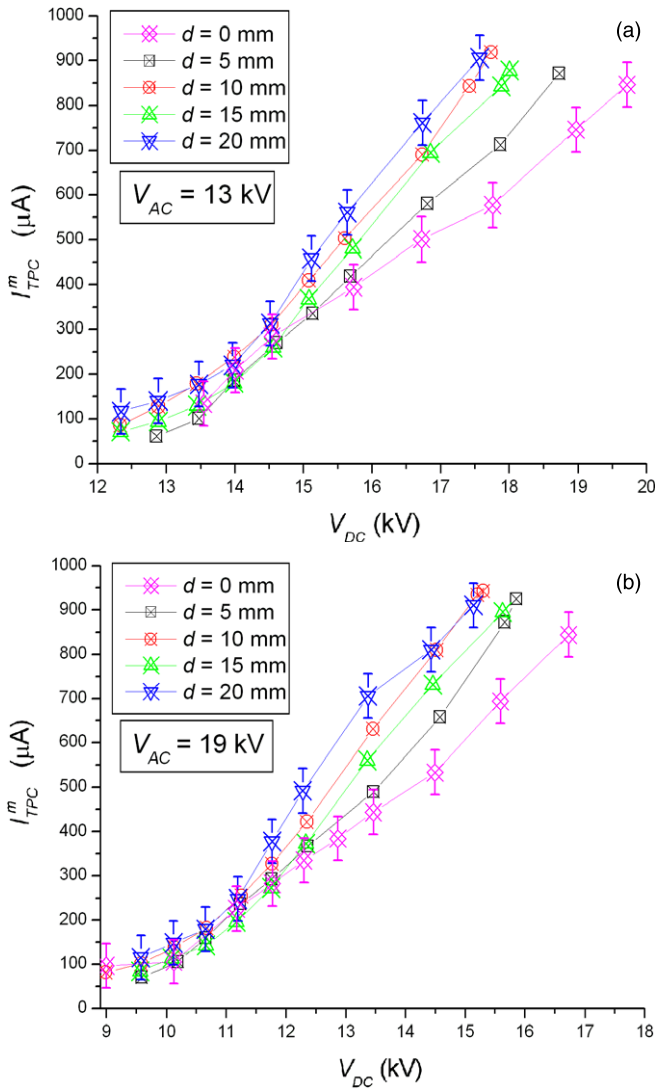

Figure 6. I^m_{TPC} as a function of V_{DC} with d as a parameter for $V_{\mathrm{AC}} = 13\,\mathrm{kV}$ (a) and $V_{\mathrm{AC}} = 19\,\mathrm{kV}$ (b).

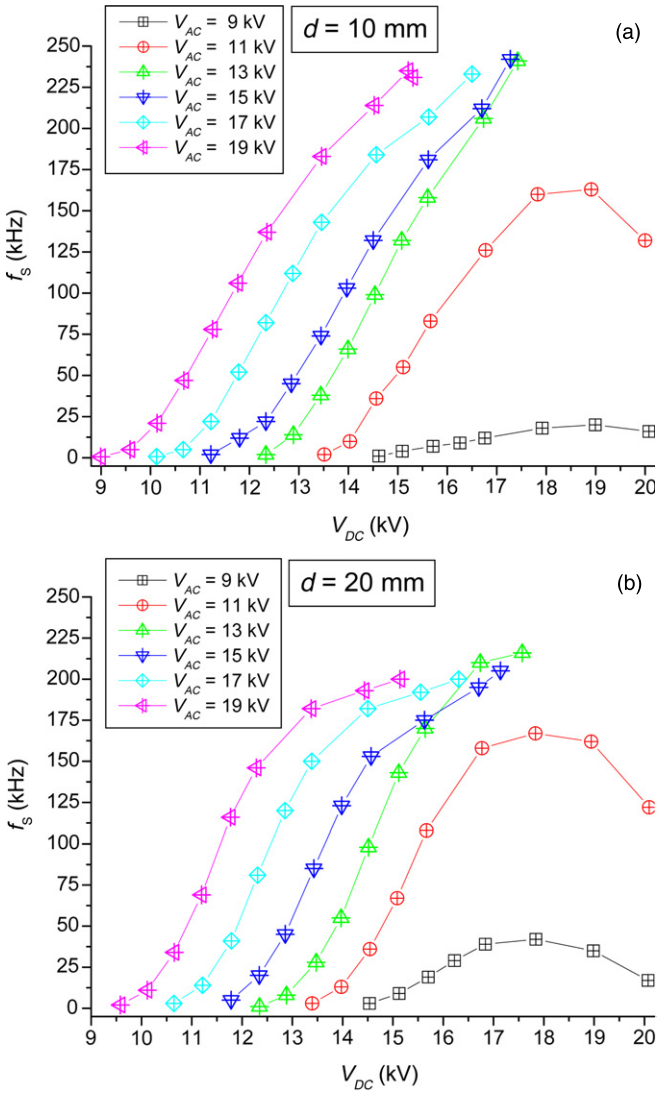

Figure 7. f_{s} as a function of V_{DC} with V_{AC} as a parameter for $d = 10\,\mathrm{mm}$ (a) and $d = 20\,\mathrm{mm}$ (b).

I^m_{TPC} (see figure 6), in this case f_{s} is remarkably independent of d. It seems that the increase in the average current for the larger d values is associated with an increase in the individual current pulse amplitudes rather than an increase in its frequency.

4. Discussion

The first point to be discussed is the operating voltage ranges necessary to establish the TPC discharge. From figure 5 the V_{DC} voltage threshold values can be identified for each considered V_{AC} voltage. For the well-developed TPC condition (i.e. $V_{\mathrm{AC}} \geqslant 13\,\mathrm{kV}$) the corresponding threshold value of V_{DC} for a given value of V_{AC} becomes larger the smaller the V_{AC} value is, resulting in a remarkably constant value of the total voltage drop between electrodes 1 and 3 at the discharge onset, $V_{\mathrm{onset}} \equiv V_{\mathrm{DC}}|_{\mathrm{thr}} + (V_{\mathrm{AC}}/2)|_{\mathrm{thr}}$ (where $V_{\mathrm{DC}}|_{\mathrm{thr}}$ and $(V_{\mathrm{AC}}/2)|_{\mathrm{thr}}$ are the respective threshold values). The constancy in the V_{onset} value ($\sim$19 kV) seems to be related to the presence of a minimum average electric field in the streamer channel necessary for its propagation across the gap (E_{c}). Note that the obtained value for this electric field threshold ($E_{\mathrm{c}} \approx V_{\mathrm{onset}}/D = 6.3\,\mathrm{kV\,cm^{-1}}$) is somewhat higher than other reported values ($\sim$3–5 $\mathrm{kV\,cm^{-1}}$) [17] but it must be taken into account that the actual $V(t)$ value for the streamer propagation is smaller than its peak value (see figure 3(b)). On the other hand, in situations where $V_{\mathrm{AC}} < 13\,\mathrm{kV}$, no stable plasma curtain could be established and the discharge presented a non-uniform structure independently of the V_{DC} applied voltage. In these cases the current discharge was much lower than that observed when $V_{\mathrm{AC}} \geqslant 13\,\mathrm{kV}$ for the same voltage drop between electrodes 1 and 3 (see figure 5). This result shows that the DBD established between electrodes 1 and 2 is essential for the existence of the TPC discharge, because it cannot be developed only by applying a voltage drop between electrodes 1 and 3 (in this case, an unstable and non-uniform plasma sheet was produced).

Another point to be discussed concerns the registered frequency values of the discharge pulses, and the relation with the temporal and spatial periodicity of the streamers. The

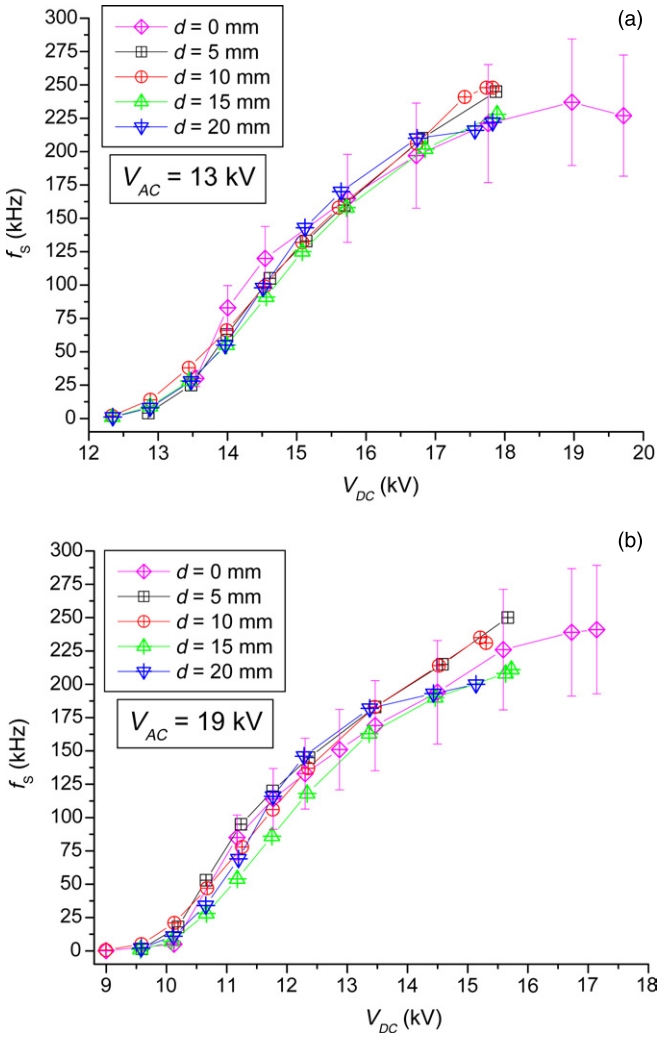

Figure 8. f_s as a function of V_{DC} with d as a parameter for $V_{AC} = 13$ kV (a) and $V_{AC} = 19$ kV (b).

temporal periodicity of a cathode-directed streamer (that is, the repetition frequency at a given spatial location) is related to the time interval (τ) required to spread out the cloud of heavy charges (positive and negative ions) that remains in the streamer channel once the streamer tip touches the cathode. This time can be estimated as

$$\tau \approx \frac{D}{\mu_i E}, \qquad (1)$$

where μ_i is the ion mobility and E the average electric field in the streamer channel ($E \approx (V_{DC} + V_{AC}/2)/D$). Using $\mu_i \sim 1.4\,\mathrm{cm^2\,V^{-1}\,s^{-1}}$ [18] and $D = 3$ cm, $\tau \approx 200$–$250\,\mu$s is obtained from equation (1) for the operating voltage ranges used in this work. On the other hand, figure 3(b) shows that the time interval during which the TPC discharge is active amounts to $\sim 50\,\mu$s. Hence, it is concluded that on average only one streamer is generated in a given spatial position during each period of the AC voltage, and its associated repetition frequency will be $\sim 5 \times 10^3$ Hz (that is, the AC frequency). The difference between this (low) value and the much higher frequency values experimentally registered (see figure 7) must be attributed to the generation of streamers at different spatial positions of the electrode during the active time of the TPC discharge. In fact, the number of concurrent streamers in each AC voltage cycle can be estimated as $n_{st} \approx f_s/f_{ac}$. The results of the experiments performed with different electrode side lengths, showing a linear dependence between f_s and this length, points to the importance of the electrode side length in the experimentally observed f_s value. According to figure 7, the number of concurrent streamers increases with the V_{DC} value (for a given V_{AC} value) up to a saturation value of $\sim$40 (200 kHz/5 kHz) that is reached just before sparking. Considering our electrode side length (15 cm) the resulting saturated number of streamers per unit length ($\sim 3\,\mathrm{cm^{-1}}$) is in good agreement with the published numerical calculations and also with experiments on multi-channel structure development in pulsed high-current sliding gas discharges [19, 20]. The increase in f_s with V_{DC} then reflects a progressive increase in the streamer density along the electrode side length, a fact that is confirmed by simple visual inspection of the discharge.

The influence of the air-gap extent (d) on the discharge behaviour (for a fixed inter-electrode distance) can be analysed from figures 6 and 8. On the one hand, figure 6(a) ($V_{AC} = 13$ kV) shows an increase in I^m_{TPC} as a function of d as long as $V_{DC} \geqslant 15$ kV, and this increase cannot be attributed to a change in the DBD intensity (since it was found that the average positive DBD current remains constant with the d and V_{DC} values). Similar behaviour was found for other V_{AC} values, but with slight changes in the V_{DC} values beyond which the increase in I^m_{TPC} is discernible (this V_{DC} value slightly decreases when V_{AC} increases, see figure 6(b)). On the other hand, figure 8 does not show an influence of d on f_s within the experimental uncertainties. This last behaviour was found for the entire range of the V_{AC} values investigated. In consequence, the change in I^m_{TPC} could be attributed to a change in the amplitude of each streamer that has a larger peak current for a larger air gap. In any case, the observed changes in I^m_{TPC} are not very large, reaching at most $\sim$40%. It is very difficult to find a comprehensive explanation for this increase in terms of the absence of the dielectric surface. In fact, several authors found that the presence of a dielectric enhances the streamer current compared with that obtained for the streamer propagation in air alone (see, for instance, [21] and references therein). The presence of a third remote electrode is the difference in this work. This electrode is the DC active cathode that promotes streamer stretching. For DC CDs it was reported that the presence of a dielectric near the active electrode affects the electric field distribution and the space charge density [22]. It is expected that similar distortions could take place in our set-up and could have some influence on the streamer propagation. Though not conclusive, this could be one of the possible candidate phenomena to which is ascribed the observed I^m_{TPC} current decrease when the dielectric was near the corona active electrode.

5. Final remarks

Based on the combination of a DBD with a CD in a three electrode system, we have presented a study of the electrical

characteristics of the TPC discharge The influence of the air-gap size (for a fixed value of the inter-electrode distance) on the discharge behaviour has also been studied. The general trend of the electrical characteristic curves (the average discharge current and the streamer frequency as functions of the AC and DC biasing voltages) was very similar for all the air-gap values considered. However, a discernible increase in the current for larger air gaps that did not have a corresponding increase in the streamer frequency was found, leading to the conclusion that in this configuration the increase in the dielectric width produces a streamer peak current decrease.

Our experimental results indicate that the development of the TPC discharge requires two conditions: (a) the presence of a positive cycle of a well-developed DBD discharge together with a CD where electrode 3 acts as the cathode and (b) a voltage drop between electrodes 1 and 3 high enough to obtain an average electric field in the gap that must exceed a minimum average electric field value in the streamer channel necessary for its propagation across the gap ($\approx$6.3 kV cm^{-1} in our experimental conditions).

Acknowledgments

This work was supported by the Argentine government grants: CONICET PIP 5378, UBACYT X-111 and ANPCYT PICT 38070.

References

[1] Goldman M, Goldman A and Sigmond R S 1985 *Pure Appl. Chem*. **57** 1353
[2] Wagner H E, Branderburg R, Kozlov K V, Sonnenfeld A, Michel P and Behnke J F 2003 *Vacuum* **71** 417
[3] Reece Roth J, Rahel J, Dai X and Sherman D M 2005 *J. Phys. D: Appl. Phys*. **38** 555
[4] Shakaran R M and Giapis K P 2001 *Appl. Phys. Lett*. **79** 593
[5] Benedikt J, Focke K, Yanguas-Gil A and von Keudell A 2006 *Appl. Phys. Lett*. **89** 251504
[6] Shoenbach K H, El-Habach A, Shi W and Ciocca M 1997 *Plasma Sources Sci. Technol*. **6** 468
[7] Rahman A, Yalin A P, Suria V, Stan O, Hoshimiya K, Yu Z, Littlefield E and Collins G J 2004 *Plasma Sources Sci. Technol*. **13** 537
[8] Ben Gadria R, Roth J R, Montie T C, Kelly-Winterberg K, Tsai P, Helfritch D J, Feldman P, Sherman D M, Karakaya F and Chen Z 2000 *Surf. Coat. Technol*. **131** 528
[9] Moreau E 2007 *J. Phys. D: Appl. Phys.* **40** 605
[10] Zastawny H, Sosa R, Grondona D, Márquez A, Artana G and Kelly H 2008 *Appl. Phys. Lett*. **93** 031501
[11] Sosa R, Kelly H, Grondona D, Márquez A, Artana G and Lago V 2008 *J. Phys. D: Appl. Phys*. **41** 035202
[12] Zouzou N, Takashima K, Moreau E, Mizuno A and Touchard G 2007 *Proc. 28th Int. Conf. on Phenomena in Ionized Gases (Prague, Czech Republic)*
[13] Louste C, Artana G, Moreau E and Touchard G 2005 *J. Electrostat*. **63** 615
[14] Manish Y 2005 Pitot tube and wind tunnel studies of the flow induced by one atmosphere uniform glow discharge (oaugdp®) plasma actuators using a conventional and an economical high voltage power supply *MS Thesis* Department of Physics , University of Tennessee
[15] Peek F W 1915 *Dielectric Phenomena in High Voltage Engineering* (New York: McGraw-Hill)
[16] Reece Roth J and Dai X 2006 *Proc. 44th AIAA Aerospace Sciences Meeting and Exhibit (Reno, NV)*
[17] Bazelyan E M and Raizer Y P 1998 *Spark Discharge* (New York: CRC Press)
[18] Raizer Y P 1991 *Gas Discharge Physics* (Berlin: Springer)
[19] Trusov K K 2006 *J. Phys. D. Appl. Phys*. **39** 335
[20] Trusov K K 2007 *J. Phys. D. Appl. Phys*. **40** 786
[21] Timatkov V V, Pietsch G J, Saveliev A B, Sokolova M V and Temnikov A G 2005 *J. Phys. D: Appl. Phys.* **38** 877–86
[22] Lee H-H and Hara M 1993 *IEEE Trans. Electr. Insul.* **28** 35–42